

ČESKÉ VYSOKÉ UČENÍ TECHNICKÉ V PRAZE  
FAKULTA DORAVNÍ

CZECH TECHNICAL UNIVERSITY IN PRAGUE  
FACULTY OF TRANSPORTATION SCIENCES

Ing. Ondřej Jiroušek, Ph.D.

APLIKACE METODY KONEČNÝCH PRVKŮ PRO STANOVENÍ  
PORANĚNÍ HLAVY PŘI DOPRAVNÍCH NEHODÁCH

APPLICATION OF THE FINITE ELEMENT METHOD FOR HEAD INJURY  
ASSESSMENT IN TRAFFIC ACCIDENTS

## Summary

The aim of the work is to demonstrate the ability of detailed finite element model of human head to quantify a head injury during traffic accident, sport injury or other traumatic event. Development of the finite element model of human skull including brain and the subarachnoidal space is shortly described. The geometry of human skull as well as that of brain is based on a sequence of Computed Tomography slices of high resolution.

The FE model reflects the real geometry of the human head with three different regions identified: (i) skull (ii) brain (iii) subarachnoidal space. In these regions four material models are defined. The human skull is modeled as a sandwich construction, composed by a thin shell of cortical bone filled with tetrahedral elements representing the spongional bone. The difference between material properties of gray and white matter is neglected and the entire brain is modeled as viscoelastic material. Subarachnoidal space is identified by means of a Boolean operation and filled with tetrahedral elements with elastic isotropic material properties prescribed.

Use of rigid body mechanics to assess either the initial conditions of the impact or acceleration time history of the center of gravity of the head is presented. As an example of a typical usage of the model a reconstruction of real world accident is presented. The injury was an accident involving a 12-year old boy on whom a handball cage fell during school sport activity. The initial conditions of the impact were obtained using a rigid body model in computer simulation of the fall. Velocities and accelerations at the instant of head hitting the ground were used as initial conditions in FE simulation of the impact using the patient specific head model.

The pressure, shear stress response, Von Mises stress response and logarithmic strain values were evaluated in frontal, parietal, occipital and midbrain regions and compared to injuries sustained. Von Mises stress was evaluated in left and right parietal regions and used for bone fracture predictions. The bone fracture was predicted at the impact side only showing good agreement with the real accident. Overall, the results from the numerical analysis were encouraging and showed good ability of the FE model to model the impact situation studied and to investigate the brain injury mechanisms.

## Souhrn

Předkládaný text pojednává o možnostech využití detailních konečnoprvkových modelů lidské hlavy pro kvantifikaci poranění hlavy např. při dopravních nehodách nebo při sportovních úrazech. Tvorba MKP modelu lidské hlavy včetně mozku a subarachnoidálního prostoru je stručně popsána. Geometrie hlavy, stejně jako geometrie mozku, jsou vytvořeny automatickými postupy na základě snímků z počítačové tomografie s vysokým rozlišením.

V MKP modelu hlavy jsou uvažovány tyto tři oblasti: (i) lebka (ii) mozek (iii) subarachnoidální prostor. Lebka je modelována jako sendvičová konstrukce, tvořená vnitřní a vnější vrstvou kortikální kosti mezi kterými je prostor vyplněn čtyřštěny reprezentujícími spongiózní kost. Pro mozek je zanedbán rozdíl mezi šedou a bílou mozkovou hmotou a celý mozek je uvažován jako viskoelastický materiál. Subarachnoidální prostor je vytvořen pomocí Booleovské operace a vyplněn čtyřštěny s lineárním izotropním materiálem.

Počáteční podmínky impaktní situace jsou stanoveny pomocí modelů uvažujícími jednotlivé části lidského těla i impaktoru jako tuhá tělesa definovaná setrvačnými vlastnostmi a navzájem spojená klouby. Jako příklad užití modelu je prezentována rekonstrukce reálného případu poranění chlapce při školní sportovní aktivitě, kdy na chlapce spadla házenkářská branka. Počáteční podmínky pohybu byly stanoveny pomocí počítačové simulace pádu. Vypočtené hodnoty rychlosti a zrychlení v okamžiku dopadu byly použity v následné MKP simulaci impaktní situace za použití modelu sestaveného z pooperačních snímků chlapcovy hlavy.

Tlak, smykové napětí, Von Misesovo napětí a logaritmické přetvoření byly vypočítány ve frontální, parietální, okcipitální a střední části mozku a porovnány s klinicky zjištěným poraněním. V levé i pravé temporální části lebky byla na základě von Misesova napětí predikována fraktura lebky. Ve shodě s klinickým zjištěním byla na straně dopadající branky modelem predikována fraktura kosti, na rozdíl od opačné strany kontaktu s povrchem hřiště, kde kost zůstala intaktní. Celkově výsledky numerické simulace prokázaly značnou schopnost detailního MKP modelu hlavy predikovat poranění lebky i mozku v reálných impaktních situacích.

**keywords**

explicit dynamics, finite element method, traffic accident, sport injury, Newmark time integration, medical imaging data, head injury criteria, intracranial pressure

**klíčová slova**

explicitní metoda integrace, metoda konečných prvků, dopravní nehoda, sportovní úraz, Newmarkova časová integrace, zobrazování v medicíně, kritéria poranění, vnitrolebeční tlak

# Contents

- 1 Introduction** **6**
- 1.1 Injury criteria . . . . . 6
  
- 2 FE model of human head** **7**
- 2.1 Introduction . . . . . 7
- 2.2 Finite element model development . . . . . 8
  - 2.2.1 Tissue segmentation . . . . . 8
  - 2.2.2 Surface reconstruction . . . . . 9
  - 2.2.3 Volumetric discretization . . . . . 10
  
- 3 Accident reconstruction** **12**
- 3.1 Introduction . . . . . 12
- 3.2 Injury description . . . . . 13
- 3.3 Rigid body modeling of the incident . . . . . 13
- 3.4 FE Model of the skull . . . . . 16
  - 3.4.1 Contact phenomena between tissues . . . . . 18
  - 3.4.2 Results . . . . . 19
  
- 4 Conclusions** **20**
  
- References** **21**

# 1 Introduction

Traumatic brain injury occurs most commonly as a result of a traffic accident, due to a fall or physical assault and it is one of the leading causes of death worldwide. Traffic accidents account for between 40 and 50 percent of all head injuries and they are also often the most serious ones. The annual number of traffic accidents is growing despite of the investment put into passive and active safety of the vehicles and in the improvement of the safety instruments and regulations. The number of traffic accidents in the Czech Republic has doubled in the last few years. The numbers are alarming: every year 1200 people die owing to traffic accidents; there are almost four-times more major injuries and perhaps twenty-times more minor injuries.

The head is one of the most frequently injured regions of human body. Despite of increasing passive safety, increasing use of seat belts and helmets it continues to be one of the major causes of death in traffic accidents. To reduce the severity of the traffic accidents, improvement of the passive safety is needed together with better understanding of the dynamic response of the human body to impact loading.

There exist two methods for investigation of the dynamic response and the injury mechanism during an impact; experimental simulation (real car crash simulations and sled tests) and numerical modeling. For the experimental simulations, the hybrid and Anthropomorphic Test Dummies (ATD) has become the industry standard for car collision testing in the last decades. Rapid advances in the computer technology and the numerical methods have enabled scientists to study problems described by a set of differential equations on very complex domains using the Finite Element Method.

## 1.1 Injury criteria

For the traumatic brain injuries, several different criteria have been used to describe their potential severity. These criteria are used not only to describe the mechanism of injury, but also to set the tolerance limits. The first widely used criterion for head injury was developed at the Wayne State University in the 1960s. The criterion was assessed using full-body cadaver tests subjected to forehead impacts on flat surface [1, 2]. Simple drop tests were performed to determine resulting linear accelerations. These linear accelerations were recorded using accelerometers mounted to the cadaver's head at the occipital region. From these experiments, first criterion for human head injuries was assessed in the form of tolerance curves, today known as WSTC - Wayne State University Tolerance Curves.

The main disadvantage of the WSTC, which uses effective accelerations as the ordinate, is that it does not reflect the effective pulse and therefore the impact duration is not taken into account. In 1971 Versace proposed Head Injury Criterion (HIC) as to enable comparisons using the mean pulse of interest. His proposed HIC was later modified by NHTSA (National Highway Traffic Safety Administration) for impacts of longer duration. This criterion is nowadays the most used criterion for head injury assessment. In 1972 it was also adopted by FMVSS (Federal Motor

Vehicle Safety Standards).

Today, the widely accepted head injury criterion is based only on the history of linear acceleration of the head. However, serious diffuse axonal injuries are most commonly caused by rotational acceleration. These injuries are caused by direct or indirect head impacts. Shear deformations originating during the rotation damage the bridging veins, leading to hemorrhaging and hematomas.

Most of the existing FE models of human head are based on a simplified geometry of the skull, brain and other structures. Another approach, presented in this work is to develop a detailed FE model of human head using CT and MRI scans of a real human head. The geometry of the human head and brain model is constructed fully automatically on the basis of the medical imaging data. This make possible to use the model for “patient-specific” reconstruction of head injuries which is an important application of these FE models. Procedures used to develop the model need minimal user intervention. On one hand this approach creates the possibility to differentiate easily between individuals, on the other hand certain structures, e.g. the bridging veins cannot be included in the model.

Presented model represents well the geometry of the skull, brain and subarachnoidal space using four material models. The sandwich construction of the human skull, composed by a thin shell of cortical bone filled with tetrahedral elements (trabecular bone) is able to reflect the behavior of the real material. With the emphasis to minimize user intervention it is impossible to make difference between material properties of gray and white matter and therefore the same viscoelastic material properties are used for the entire brain.

Tetrahedral elements are used to fill all three regions within the human head (skull, brain and subarachnoidal space). The main advantage of using the tetrahedral elements is that these models can be generated in short time almost automatically on basis of a sequence of medical images of high resolution. This would enable for post-traumatic assessment of brain injuries e.g. in case of traffic, sport or daily-activity accidents.

## **2 FE model of human head**

### **2.1 Introduction**

Human head is too complicated to be well represented by a simplified geometry defined as a set of geometrical primitives. Therefore, presented FE model was built using CT and MRI scans of human head taken in resolution 512x512 pixels at 1 mm distance. Special attention was paid to develop the geometry of the human head automatically avoiding manual adjustment of the model. This is important when there is a need for patient-specific models, e.g. in reconstruction of real world injury as it is illustrated in chapter 3 dealing with reconstruction of a sport accident. Great emphasis was paid to minimize the number of poorly shaped elements in the mesh, because the model is used in explicit finite element code using reduced integration scheme and linear shape functions.

## 2.2 Finite element model development

Sophisticated image processing techniques are used to differentiate between the various tissues presented in the head. The model is reconstructed from the volumetric medical data using Marching Cubes Algorithm (MCA, [3]), decimation algorithm [4] and Delaunay tetrahedralization [5] approach. During the reconstruction process additional algorithms, e.g. mesh smoothing using Laplace operator are used to smooth and optimize the resulting FE mesh.

### 2.2.1 Tissue segmentation

The first task in the reconstruction process is the tissue segmentation, i.e. selection of the tissue of interest in the sequence of medical images. For the segmentation of the bone tissue CT images taken at 1 mm intervals of 512x512 pixel resolution were used. There are several different techniques used: intensity based segmentation, edge detection techniques, region growing techniques. Traditional intensity based segmentation is suitable for images of high quality where every tissue of interest is well separated from each other. These algorithms relies on the fact, that pixels representing the same tissue are clustered around a mean characteristic value. This holds well e.g. for computer tomography used in reconstruction of the cortical bone, but is not suitable for MRI images that have inhomogeneities which give us smoothly varying, nonlinear field. The effect of noise is usually reduced using low-pass filters (Fourier low pass filter, real space averaging or median filter) or high-pass filters (Gaussian high-pass filter, high-pass Butterworth filter).

Using traditional thresholding techniques we often gain misclassified regions in the image. The simplest way to find the specific tissue of interest is to convert input image using *thresholding*, i.e. one-bit quantization. Thresholding determines a unique range of physical values for each pixel that corresponds to the tissue of interest. Because of the high quality of the input CT images, simple intensity based segmentation was found suitable for the bone tissue. Series of segmented images is presented in Fig. 1.

Threshold-based segmentation method is normally not effective for MRI image. For the brain tissue segmentation, segmentation using active contours (region growing) had to be used because inhomogeneities in the MRI scans give us smoothly varying, nonlinear fields in the images. Region growing identifies regions of interest within an image based on an attempt to match the image to a parametric edge model.

The advantage of region growing techniques is that it provides continuous boundaries for regions of interest. A snake model has the advantage over edge-detecting approaches for segmentation in that no edge linking is required. The key idea is to define a set of control points (snaxels) and propose an evolutionary model to attract the snake toward the desired boundaries of the region of interest.

The snake is defined as contour  $\mathbf{w}(s) = (x(s), y(s))^T$  with a functional (usually a sum of internal and external energy):

$$\mathcal{I}(\mathbf{w}) = E_{int}(\mathbf{w}) + E_{ext}(\mathbf{w})$$



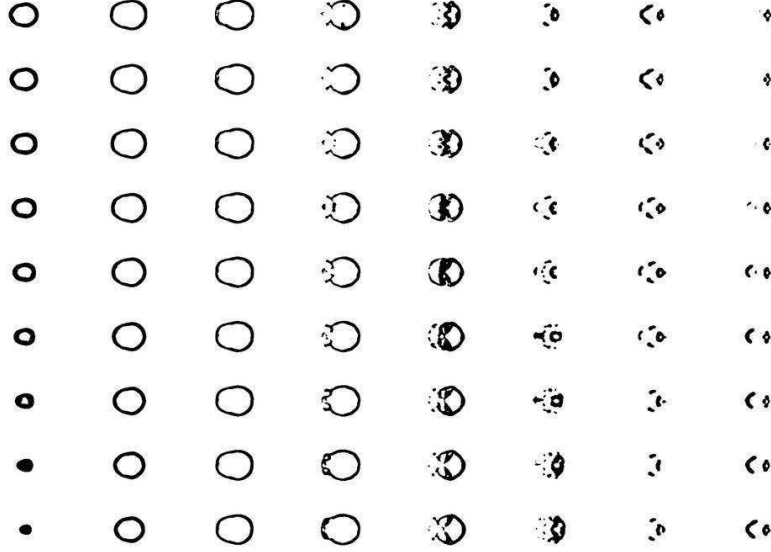


Figure 1: Segmentation of the skull tissue in the series of CT scans

Internal deformation energy of the flexible contour can be defined as:

$$E_{int}(\mathbf{w}) = \int_0^1 \xi(s) \left| \frac{\partial \mathbf{w}}{\partial s} \right|^2 + \zeta(s) \left| \frac{\partial^2 \mathbf{w}}{\partial s^2} \right|^2 ds$$

External energy (scalar potential function defined on the image):

$$E_{ext} = \int_0^1 -c |\nabla [G_\sigma \odot I(x, y)]| ds$$

To establish the final deformed position of the snake is equal to finding the minimum of  $\Pi$  (solving Euler-Lagrange equation for  $w$ ):

$$-\frac{\partial}{\partial s} \left( \xi \frac{\partial \mathbf{w}}{\partial s} \right) + \frac{\partial^2}{\partial s^2} \left( \zeta \frac{\partial^2 \mathbf{w}}{\partial s^2} \right) + \nabla P(\mathbf{w}(s, t)) = 0$$

These methods are very useful when there exists a-priori idea of the shape of the object to be found. They are very robust in case of images of poor quality (ultrasound pictures) or finding an object that does not create big differences in the pixel intensity but its shape is known (e.g. tumor detection). The starting template and the final position of the snake used in segmentation of the brain is presented in Fig. 2.

### 2.2.2 Surface reconstruction

After the segmentation of both the skull and brain tissue, the inner and outer surfaces of both parts were reconstructed using the Marching Cubes Algorithm (MCA, [3]). As the result of the MCA, we obtain very large number of triangles describing the surface of the domain of interest. To be able to use this geometrical representation of the domain later in the FE simulations,

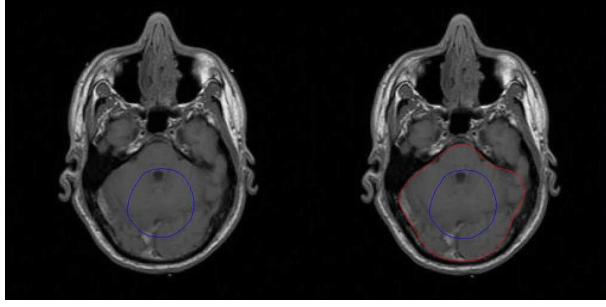


Figure 2: Snake model used for brain segmentation

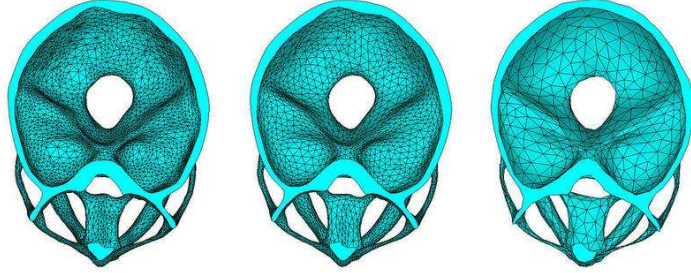


Figure 3: Decimation of the skull mesh (i) 200,000 (ii) 50,000 (iii) 5,000 elements

it is necessary to reduce the number of triangles to a reasonable number using a decimation algorithm (see e.g. [4]. Out-of-plane distance decimation and border-distance decimation were used for repetitive removal of vertices from a triangular mesh in order to reduce the density of the mesh in places where they are not necessary for the surface description. Surface mesh optimization using energy minimization approach was used to optimize the final mesh. This approach helps to balance two contradictory goals - resulting mesh with fewer vertices than the original one while keeping the geometry close to the original model.

The original surface mesh obtained by the MCA consisted almost of 1,500,000 triangles (both outer and inner surfaces were reconstructed). Due to the high density of the mesh, figure showing this too dense model is not shown. Fig. 3 shows FE models with different density obtained after several steps of decimation. The first model obtained had more than 200,000 elements. Loosening the decimation criteria it was possible to reduce the number of elements describing the skull to less than 5,000.

### 2.2.3 Volumetric discretization

After successful decimation one has the surface of the model represented by a set of closed triangular elements. The last step is to create volumetric representation of the object from this surface representation. Naturally, it is convenient to use tetrahedral elements. However, if, for some reason we would need to use hexahedral elements, there is still a possibility to convert each tetrahedra in the mesh into four hexahedral elements. It is unfortunately impossible to obtain hexahedral mesh of such a complicated domain as in this case of human skull.

For the discretization of the volume Delaunay triangulation [5] in 3-D is used. The Delaunay

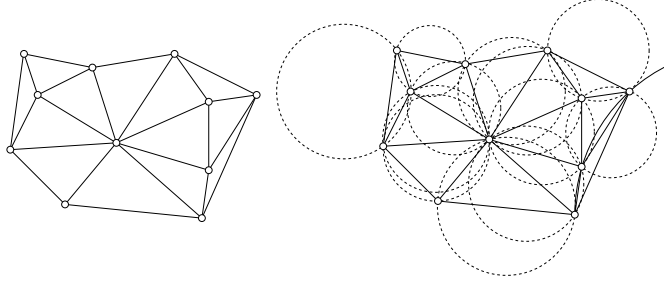


Figure 4: Delaunay "empty circle" criterion

triangulation is one of the methods for subdivision of an area into triangles or in 3-D volume into tetrahedrons. The Delaunay criterion (Fig. 4), sometimes called the "empty circle" or "empty sphere" property, says that any node must not be contained within the circle (or circumsphere) of any triangle (tetrahedra) within the mesh. A circumcircle (circumsphere) can be defined as the circle (sphere) passing through all three (four) vertices of a triangle (tetrahedron). The Delaunay triangulation of a given point set is the dual structure of its Voronoi diagram [6] and can be obtained using this Voronoi diagram. The Voronoi diagram has following property. For each site every point in the region around that site is closer to that site than to any of the other sites. For more information about the Voronoi diagrams and Delaunay triangulations see e.g. [7]. In our case result of the Delaunay triangulation (tetrahedralization) is a set of tetrahedra filling the entire 3-D domain.

Delaunay triangulation used for the discretization of the volume does not guarantee elements with good aspect ratios. The resulting mesh can contain elements of bad shape that can slow down the solution or produce undesirable errors. The Delaunay triangulation must be therefore followed by mesh optimization to avoid sliver elements (elements with very small spatial angle between two sides) as well as other elements of bad shape. Three methods used to improve the quality of existing tetrahedral mesh are used: (i) mesh smoothing, (ii) nodal points insertion and deletion and (iii) local re-meshing.

To smooth the mesh, Laplacian smoothing is used. It is a straight-forward method derived from a finite difference approximation of the Laplace operator. A vertex in the mesh is moved to the centroid of the surrounding (topologically connected) vertices:

$$P_{new} = \frac{1}{n} \sum_{i=1}^n \alpha_i P_i$$

If a set of surrounding mesh vertices forms an extremely non-convex polygon its center of mass may lie outside the polygon. In such a case overlapping elements would be generated and therefore the mesh vertex is skipped. Laplacian smoothing results in more homogeneous meshes – therefore it is suitable when elements of approximately the same size are required.

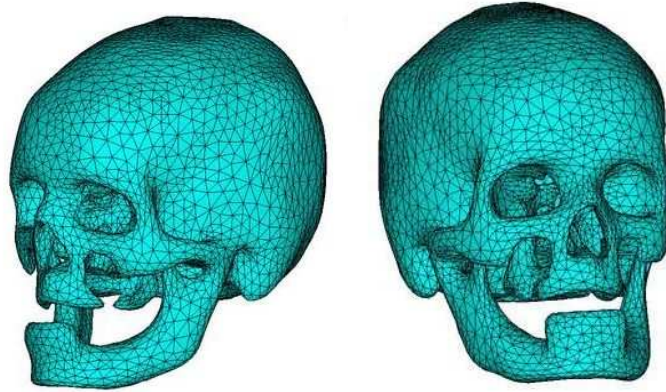


Figure 5: FE model of the human skull

### 3 Accident reconstruction

#### 3.1 Introduction

Application of the FE model of skull and brain in reconstruction of a sport accident demonstrates the ability of such FE model to predict injuries sustained during e.g. traffic accident. A complete understanding of injury pattern and the underlying biomechanics of the injury can describe the cause of the injury or to assess limits of forces acting upon human body during the incident. Models can be used to describe critical factors such as the position and posture of a person during the incident or e.g. direction from which the acting force was applied at the time of injury. These factors are often important also in the field of forensic biomechanics.

The methods used to reconstruct an injury or accident use principles of theoretical mechanics to understand basic processes and mechanisms related to the structure and function of bone as well as other skeletal tissues. In sport biomechanics as well as in forensic biomechanics, human body kinematics and kinetics are evaluated and described, as well as the injury mechanisms. The reconstruction usually involves review of medical documentation describing the injuries, inspection of the accident site and modeling of the injury or accident itself. Application of rigid body modeling using a pedestrian model in a reconstruction of a traffic accident is shown in Fig. 6. The kinematics of the body hit by a car at 50 km/h was obtained using the 50% male pedestrian model.

In the study a rigid body model of the human body involved in the accident was used to assess initial conditions which were later used in finite element modeling of the head impact. From the rigid body modeling a comparison of different approaches to head injury prediction is drawn. Results are compared to finite element simulation using presented FE model subjected to initial conditions obtained from rigid body simulation just before the head impact with the ground. Head injury criterion as proposed by Miller et al. in [8] is applied. The pressure, shear stress response, von-Mises stress response and logarithmic strain values were evaluated in four regions: (i) frontal, (ii) parietal, (iii) occipital and (iv) midbrain region. Results from the numerical

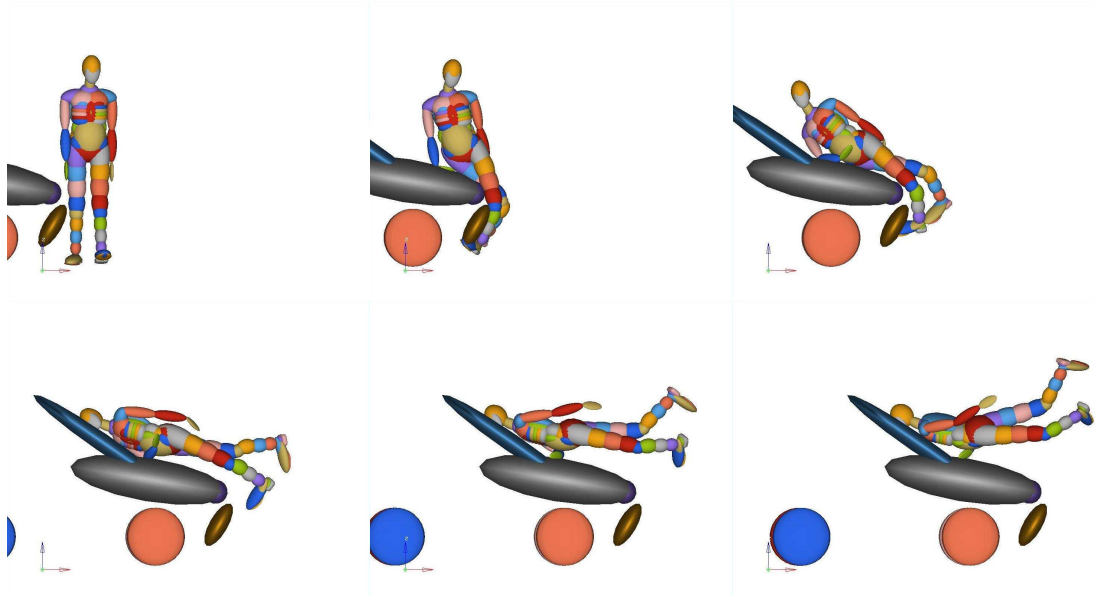


Figure 6: Reconstruction of a traffic accident

analysis of the accident showed good agreement with clinically observed head injuries.

### 3.2 Injury description

The aim of the reconstruction was to develop a FE model that would be able to characterize the mechanics of the real injury. The injury to be reconstructed was a sport accident involving a 12-year old boy on whom a handball cage fell during school sport activity. The boy fell immediately unconscious and was hospitalized shortly after the accident, with impressive fracture in temporal-parietal region of the left hand side of the skull. Dilatation of dura and the brain tissue at the side of impact, hemorrhagic contusion of basal ganglia, traumatic subarachnoidal bleeding and two lacerated wounds – one frontal and the second parietooccipital brain region. The fracture of the skull was almost one third of the hemisphere in length and sharp fragment of the skull caused the underlying dura dilatation.

Surgical treatment of acute, traumatic, compressive haematoma consisted in craniotomy, sanitation of contusions, evacuation of the epidural haematomas and plastic surgery of dura and calva. Intracranial pressure was monitored using a pressure gauge. On the seventh day after the surgery, the boy was transferred to spontaneous ventilation, extubated. Today the boy is undertaking rehabilitation and logopedic care, because hard perceptive hypacusia was diagnosed postaccidentally. Two months after the accident, the boy is attending a grammar school in place of residence with personal assistant.

### 3.3 Rigid body modeling of the incident

The initial configuration of the head impacting the ground as well as the initial velocity of the steel cage were obtained from rigid-body modeling of the fall. For the rigid-body simulation

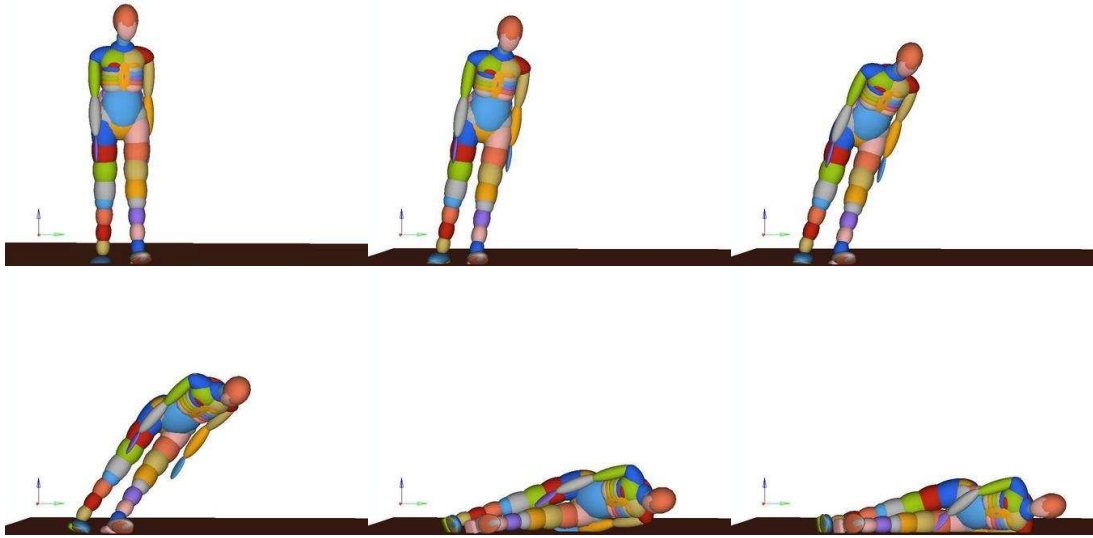


Figure 7: Reconstruction of the fall accident (case 1: falling sideways)

MADYMO software package was used in which a distinction between occupant models, pedestrian models and detailed segment models is made. The accident was reconstructed using the MADYMO 5% female pedestrian model. The outer geometry of the pedestrian models is represented by ellipsoids, which provide a less accurate representation of the geometry but result in shorter computation times than facets. Inertial properties of all segments are incorporated in the rigid bodies of the pedestrian models. In the ellipsoid pedestrian models, structural deformation of flexible components is lumped in kinematic joints in combination with dynamic restraint models. This approach was applied in order to simulate elastic long bone bending as well as fracture in femur and tibia. Deformation of soft tissues (flesh and skin) is represented by force-penetration based contact characteristics for the ellipsoids. These characteristics are used to describe contact interactions of the pedestrian model with itself and with its environment.

The small female model (1.52 m and 49.8 kg) was closest in weight and size to the boy injured (1.58 m and 40 kg). From the female model, the ellipsoids representing breasts were removed. The model was subjected only to gravitational acceleration, the initial configuration is depicted on the first image of the series presented in Fig. 7.

The model is equipped with sensors located in 16 important places registering position, velocity, acceleration and force in every time instant. For the accelerations, acceleration field model calculating forces at the centers of gravity of bodies due to a homogeneous acceleration field is used.

From the rigid body simulation of the fall several important values can be easily determined, e.g. acceleration of the center of gravity of the head. From the resultant acceleration history we can calculate the head injury criterion for the studied free fall as described previously in chapter ??.

Several injury parameters, namely  $HIC_{36}$  and  $HIC_{15}$  were calculated from the acceleration history. Resulting head injury criterion values were same for 15 ms and 36 ms time window:

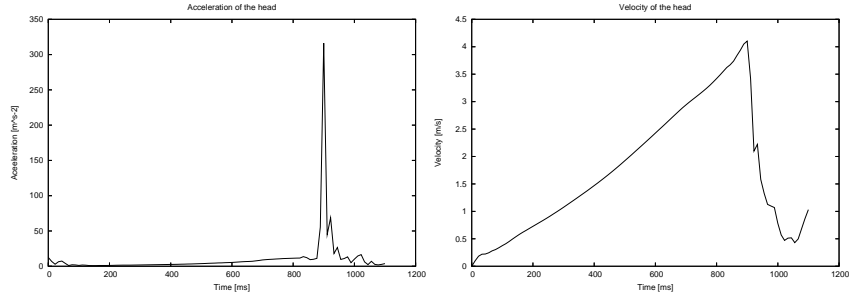


Figure 8: Acceleration and velocity history for the first case

component	time [s]	min velocity [ $\frac{m}{s}$ ]	time [s]	max velocity [ $\frac{m}{s}$ ]
(sum)	0.00	0	900.20	4.1040
x-comp.	913.50	-1.0522	932.60	0.5033
y-comp.	5.10	-0.0007	861.40	1.7217
z-comp.	910.10	-3.7538	913.70	2.2213

Table 1: Peak velocities of the head CoG (first case)

component	time [s]	min accel [ $\frac{m}{s^2}$ ]	time [s]	max accel [ $\frac{m}{s^2}$ ]
(sum)	–	–	912.10	4553.5
x-comp.	912.00	-1499.3	911.30	557.12
y-comp.	912.10	-4079.9	914.20	447.22
z-comp.	912.20	-1410.6	920.40	167.59

Table 2: Peak accelerations of the head CoG (first case)

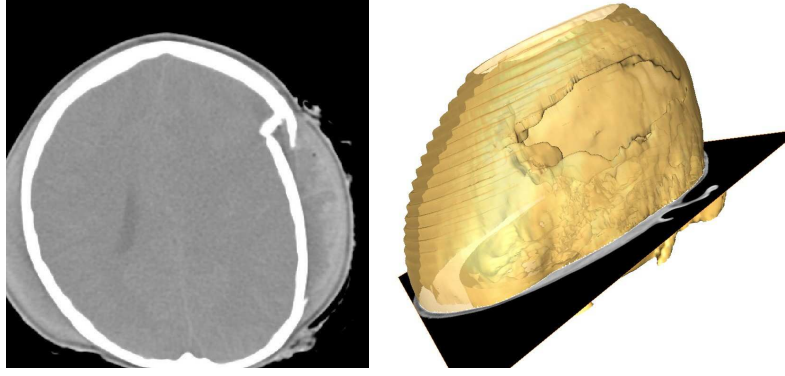


Figure 9: pre-operation situation: (a) CT-image (b) reconstructed surface

${}^1\text{HIC}_{36}=3562,5$  ( $t_1 = 911.30$  ms,  $t_2 = 912.70$  ms) and  ${}^1\text{HIC}_{15}=3562,5$  (using the same time window). Beside HIC, linear and angular acceleration peak values were used for injury criteria determination. The values of linear acceleration were above the lower bound for contrecoup contusion, subarachnoidal haemorrhage and subdural haematoma. The values were also above the 100% concussion probability.

To conclude, the 5% female pedestrian model was used to assess initial conditions of the head at the time of impact with the ground to be later used in the finite element simulation using the detailed FE model of the boy's head. The components of velocity and acceleration at the time of impact obtained at the center of gravity of the pedestrian head were imposed on the detailed FE model. To determine the velocity and angular acceleration of the impacting handball cage a simple rigid model was used. To calculate center of gravity and inertial properties of the cage needed for solution of partial differential equation of motion a model using beam elements of appropriate sectional and inertial properties was built using ANSYS preprocessor.

The cage was supposed to fall from its indifferent equilibrium position. Differential equation of motion  $I\ddot{\varphi} - mgy_T \sin \varphi(t) = 0$  was used to determine velocity and angular acceleration of the upper bar of the cage at the moment it hit the boy's head. Solution of the differential equation is not trivial, it leads to an elliptic integral. Therefore, the equation was linearized and solved incrementally for  $\varphi$  to be sufficiently small (increment of  $5^\circ$  was assumed). The components of velocity and acceleration determined from the equation of motion for the angle  $\varphi = 84.5^\circ$  (upper bar touching the skull) were used as initial conditions for the movement of the cage modeled as deformable bar in the FE analysis of the accident.

### 3.4 FE Model of the skull

CT data of the patient's head were used to develop a detailed FE model for the simulation. CT images of the head were taken both pre- and postoperatively. From the pre-operative images it was possible to reconstruct the damaged skull. The open fracture of the skull and the huge haematoma presented on the impacted site are clearly visible in Fig. 9.

The geometry of the model was prepared based on the post-operative images. The surface of



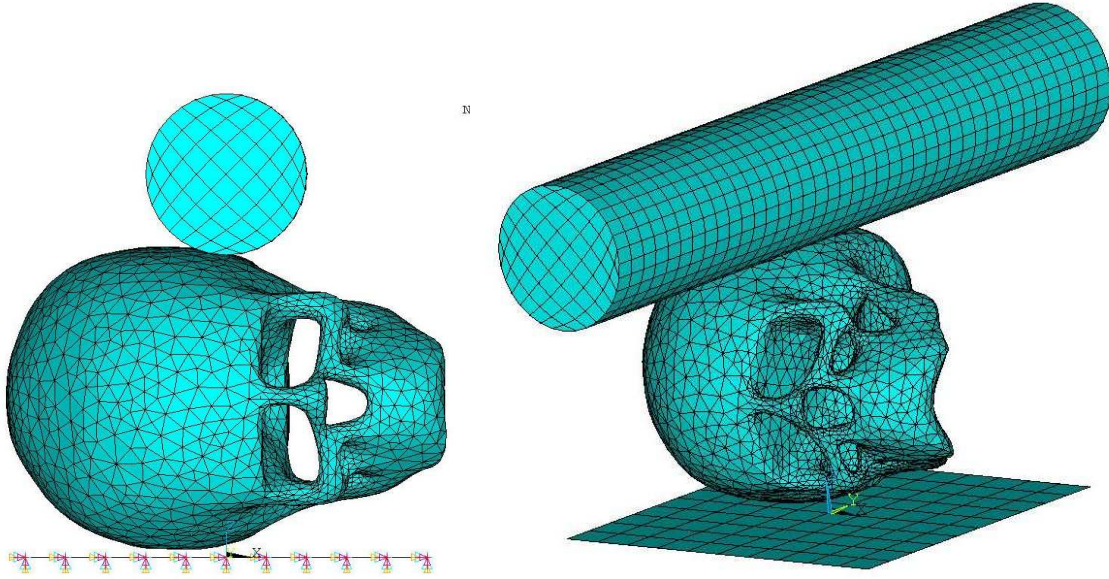


Figure 10: FE model of the handball cage accident

the brain was reconstructed based on the same series of CT images because MRI data were not available. The outlines of the brain in the whole set of CT-images were therefore defined by shrinking the inner outline of the skull and hence representing reduced intracranial region.

Within the FE model of the head four different regions were defined:

- skull, represented by volumetric tetrahedral elements for the spongional bone covered by inner and outer layer of shell elements for cortical bone of uniform thickness of 1 mm. Spongional bone was modeled as elasto-plastic, with following material properties: Young's modulus of elasticity  $E_{spon}=2.200$  MPa, Poisson ratio  $\nu=0.01$ , material density  $\rho=1500 \frac{kg}{m^3}$ , ultimate strength in compression  $\sigma_{ult}^- = 32$  MPa, ultimate strength in tension  $\sigma_{ult}^+ = 30$  MPa. Cortical bone was considered elasto-plastic as well with following material properties:  $E=12.000$  MPa,  $\rho=1850 \frac{kg}{m^3}$ ,  $\nu=0.21$ ,  $\sigma_{ult}^- = 80$  MPa,  $\sigma_{ult}^+ = 140$  MPa
- brain, modeled as viscoelastic material, no differentiation between material properties of white and gray matter was considered. Bulk modulus was set to  $K=2200$  MPa, density of the brain tissue is close to that of water  $\rho=1000 \frac{kg}{m^3}$ , instantaneous shear modulus  $G_0=1.036$  kPa, and the shear modulus at infinity  $G_\infty=0.0185$  kPa, reciprocal decay coefficient  $\frac{1}{\beta}=0.0165 \frac{m}{s}$ .
- subarachnoidal space which is filled with the cerebrospinal fluid (CSF) is the main shock absorber and is composed mainly from water (99%). In this study, the subarachnoidal space is modeled with bulk modulus  $K=0.105$  MPa, shear modulus  $G=1.086$  MPa, density  $\rho=1130 \frac{kg}{m^3}$  and Poisson ratio  $\nu=0.495$ .

The situation modeled was set according the accident: the boy's head touching the ground and the cage cross-bar falling on the left part of the head, see Fig. 10.

The playground is covered with the CONIPUR material, which is an impact absorbing, permeable layer of polyurethane, often used for playground surfaces and for these purposes it is approved by Swiss Sport Institute and International Knowledge of Sport Surfaces Association. The surface was modeled using three layers of solid elements with elasto-plastic material properties with following constants: Young's modulus 4209 MPa, yield strength 132 MPa, density  $\rho=1050\frac{kg}{m^3}$ , Poisson's ratio  $\nu=0.41$ .

The cage was modeled as a bar of the same cross-sectional properties as the real one, but only the upper bar was modeled. The density of the bar was scaled as to represent the overall force exerted to the head in the moment of contact. The cage is made of zinc-coated steel with following material properties (elasto-plastic material): Young's modulus 195 GPa, yield strength 230 MPa, density  $\rho=8030\frac{kg}{m^3}$ , Poisson's ratio  $\nu=0.3$ .

### 3.4.1 Contact phenomena between tissues

The importance of modeling contact conditions between all the tissues presented in human head has been studied by many authors, e.g. [9], [10]. The effects of contact are focal and localized and it is widely understood that contact effects contribute little to brain diffuse injuries. For instance, Ommaya and Hirsch in their paper from 1971 [10] concluded that if head rotation were the crucial brain injury mechanism, cerebral concussion would be produced at an identical threshold for rotational velocity of the head irrespective of how the head rotation was induced, i.e. directly or indirectly. Their experimental data did not support this and showed a significant contribution to the brain injury by the local effects of impact.

In this study a direct contact impact is modeled. For this reason the cranium cannot be assumed rigid as it is in many studies studying response of human brain to e.g. rotational or linear acceleration as in [11]. Moreover, the cranium plays a key role in studying this so-called open-head injury. The impact delivered to the head is transferred through the cortical layer to the spongy bone and through the inner layer of cortical bone to intracranial space. The intracranial space is filled with CSF. It was found, that for modeling of intracranial pressure response, beside the effects of skull topology, CSF depth is an important factor. Careful consideration was therefore taken to precise tissue segmentation of the region to ensure appropriate thickness of the subdural space is ensured.

Contact defined between the brain and skull was therefore defined as sliding with friction. Between the inner surface of the skull and the CSF layer, sliding is allowed while separation of the contacting brain and CSF layer is allowed. This makes gap formation at the CSF-cerebrum interface possible. For all interfaces, contact with sliding and friction (friction coefficient 0.2) was modeled as proposed by Miller et al. in 1998 (see [8]).

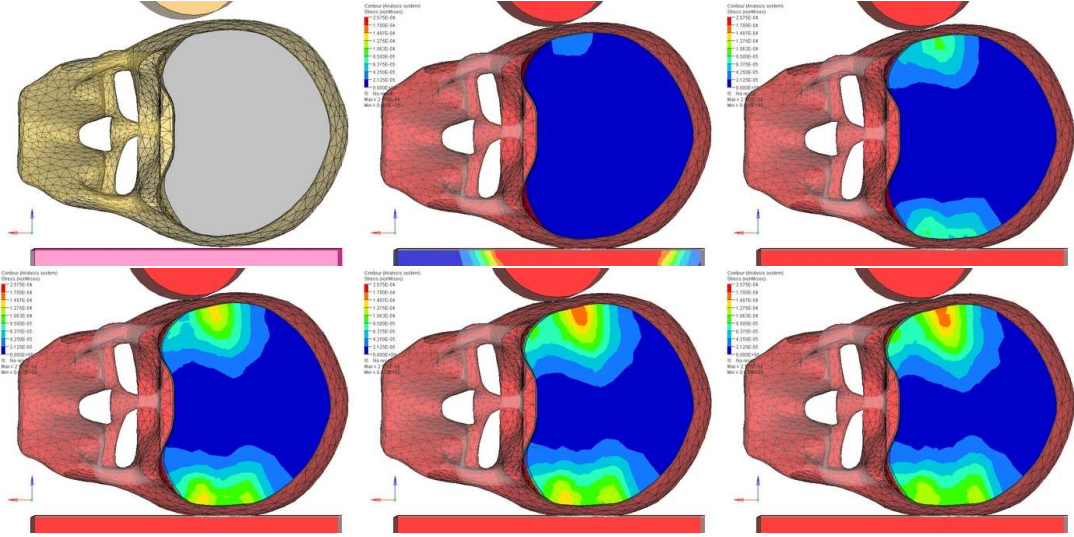


Figure 11: von Mises stress in the brain tissue in 0, 2, 4, 6, 10 ms time intervals

### 3.4.2 Results

The aim of the study was to model the accident using explicit finite element model and to assess the possibilities of the existing injury criteria to describe the lesions caused by the falling cage. Remarkable observation in the study was the fact, that the skull was fractured at the side of the impact with the cage only, whereas on the opposite side, at the contact with ground it remained intact. Also brain injuries on the side opposite to cage impact were not so severe as on the opposite side. Obvious explanation of this phenomena is that the playground was covered with 16 mm layer of cushion material (CONIPUR 2S) absorbing much of the deformation energy of the reverse side.

For the FE modeling of the impact conditions, explicit dynamics solver LS-DYNA is used. The solution of an explicit problem is stable only if the time increment  $\Delta t$  is smaller then the critical one. The critical time increment can be calculated based on the Courant–Friedrichs–Levy criterion and for stability reasons is lowered by a scale factor of 0.9 to  $\Delta t = 0.9 \frac{l}{c}$ , where  $l$  is the characteristic length of an element and  $c$  is the propagation velocity. The time step was held constant during the simulation. Reduced (one–point) integration together with viscous hourglass control was used for faster element formulation. The use of one–point integration is advantageous due to savings on computer time and in case of large deformations of the brain.

Contact conditions were prescribed between the brain and inner surface of the skull as well as between the outer surface of the skull and the rigid plate. As an illustrative example of the results the fields von Mises stress in the brain tissue (Fig. 11) are presented.

Prediction of skull fracture was based on Yoganandan et al. [12] experimental results where the force necessary to fracture cadaver skulls ranged between 8.8 kN and 14.1 kN, with an average of 11.9 kN. The authors also concluded, that for the fixed head the force–deflection curve was found to be insensitive to impact location. The peak force from the MADYMO simulation was

7.4 kN indicating no skull fracture. In this case, the falling cage is not modeled and the peak force is obtained from the free fall only. This indicates that in case of free fall no skull fracture would occur. On the other hand, results from the finite element modeling show peak force more than double of that value clearly predicting skull fracture.

Results from the FE modeling were used for tissue thresholds. Most of the thresholds are used for axonal injury prediction rather than whether a particular type of injury would occur ([13]). In recent years few works with injury thresholds based on von Mises stress appeared, particularly the work of Willinger et al. [14] and Baumgartner [15].

In this work the injury limits were set according to recent work of Baumgartner and Willinger [16]. The thresholds were derived from a FE modeling of 64 accident involving helmeted motorcyclists, American footballers and pedestrians. The limits were set to 20 kPa for concussion, and 40 kPa for severe brain neurological lesions. The limit for subdural and subarachnoidal haematoma sets the global strain energy of the subarachnoidal space to 5 J. A global strain energy of the skull of 2 J leads to skull fractures.

Using presented FE model von Mises stress was evaluated at the side of impacting cage, at the opposite side (temporal regions) as well as at the occipital and parietal and midbrain regions. In the temporal regions the peak values of von Mises stress were 47 kPa and 23 kPa clearly predicting brain lesions and haematomas on both sides. Using these limits in our case of falling handball cage, the skull fracture was predicted with global strain energy of the skull reaching 4.3 J. The global strain energy of the subarachnoidal space was more than 8 J suggesting subdural haematomas.

## 4 Conclusions

Techniques used to develop patient-specific finite element human head model based on a series of CT images of high resolution were presented. The medical image data were transformed into a three-dimensional FE model and implemented into the explicit finite element code ANSYS LS-DYNA. The model was used in reconstruction of an accident which lead to serious skull and brain injuries.

The model consists of three-layered skull (cortical and trabecular bone), subarachnoidal space and brain. Tetrahedral elements are used to fill all three regions defined in the model. Procedures used to develop such a model based on medical imaging data are fully automatic and require minimal user intervention. This make possible to use the model for “patient-specific” reconstruction of head injuries which is an important application of these FE models. Procedures used to develop the model need minimal user intervention. On one hand this approach creates the possibility to differentiate easily between individuals, on the other hand it keeps the model relatively simple, not accounting for certain inner structures. With the emphasis to minimize user intervention it is impossible to make difference between material properties of gray and white matter and therefore the same viscoelastic material properties are used for the entire brain.

The initial conditions of the impact were obtained using a rigid body model in computer simulation of the fall. Velocities and accelerations at the instant of head hitting the ground were used as initial conditions in FE simulation of the impact using the patient specific head model. The use of rigid-body modeling and pedestrian models is a fast tool to reconstruct the kinematics of a traffic accident, sport accident or daily activity injury. With a detailed FE model of human head it is possible to obtain the stresses origination in the tissues from loading assessed by the rigid-body simulation.

Presented reconstruction of the handball accident was used to demonstrate the ability of detailed FE models to replicate an accident, in this case a cage falling on a handball player's head. The bone fracture was predicted at the impact side only showing good agreement with the real accident. Overall, the results from the numerical analysis were encouraging and showed good ability of the FE model to model the impact situation studied and to investigate the brain injury mechanisms.

Without such a detailed FE model of the head, only the force and accelerations obtained from a rigid-body analysis are compared to the resulting injury. The stress and strain levels are by far better indicators of brain injury or skull fracture. However, the tolerance limits in terms of strain and stresses are fewer than those expressed in terms of acceleration. Further experimental investigations are needed to assess the new tolerance limits for various impact conditions.

## References

- [1] E. S. Gurdjian, J. E. Webster, and H. R. Lissner, "Observations on the mechanism of the brain concussion, contusion, and laceration," *Surg Gynecol Obstet*, no. 101, pp. 680 – 690, 1955.
- [2] H. R. Lissner, M. Lebow, and F. G. Evans, "Experimental studies on the relation between acceleration and intracranial pressure changes in man.," *Surg Gynecol Obstet.*, vol. 11, no. 111, pp. 329 – 338, 1960.
- [3] W.E. Lorensen and H.E. Cline, "Marching Cubes: A High Resolution 3D Surface Construction Algorithm," *Computer Graphics*, vol. 21, pp. 155–168, July 1987.
- [4] W.J. Schroeder and J.A. Zarge, "Decimation of Triangle Meshes," *Computer Graphics*, vol. 26, pp. 65–70, Aug. 1992.
- [5] Tsung-Pao Fang and Les A. Piegl, "Delaunay Triangulation in Three Dimensions," *IEEE Computer Graphics and Applications*, vol. 15, Sept. 1995.
- [6] S. Fortune, "A sweepline algorithm for voronoi diagrams," *Algorithmica*, vol. 2, pp. 153 – 174, 1987.
- [7] S. Fortune, "Voronoi diagrams and delaunay triangulations," *Algorithmica*, vol. 1, pp. 193 – 234, 1992.
- [8] R. Miller, S. Margulies, M. Leoni, M. Nonaka, X. Chen, D. Smith, and D. Meaney, "Finite element modeling approaches for predicting injury in an experimental model of severe diffuse axonal injury," in *42th Stapp Car Crash Conf*, no. SAE Paper No. 983154, pp. 155 – 166, 1998.

- [9] A. Ommaya and T. Gennarelli, "Cerebral concussion and traumatic unconsciousness," *Brain*, no. 97, pp. 633 – 654, 1974.
- [10] A. K. Ommaya and A. E. Hirsch, "Tolerances for cerebral concussion from head impact and whiplash in primates," *Journal of Biomechanics*, no. 4, pp. 13 – 31, 1971.
- [11] D. W. A. Brands, *Predicting brain mechanics during closed head impact: numerical and constitutive aspects*. PhD thesis, 2002.
- [12] N. Yoganandan, F. A. Pintar, A. Sances, P. R. Walsh, C. L. Ewing, D. J. Thomas, and R. G. Snyder, "Biomechanics of skull fracture," *J Neurotrauma*, vol. 12, no. 4, pp. 659 – 668, 1995.
- [13] B. I. Morrison, H. L. Cater, C. Wang, F. C. Thomas, C. T. Hung, G. A. Ateshian, and L. E. S. L. E., "A tissue level tolerance criterion for living brain developed with an in vitro model of traumatic mechanical loading," *Stapp Car Crash Journal*, no. 47, pp. 93 – 105, 2003.
- [14] R. Willinger, D. Baumgartner, B. Chinn, and M. Neale, "Head tolerance limits derived from numerical replication of real world accidents," in *IRCOBI Conf., Montpellier*, pp. 209 – 221, 2000.
- [15] D. Baumgartner, R. Willinger, N. Shewchenko, and M. Beusenbergh, "Tolerance limits for mild traumatic brain injury derived from numerical head impact replication," in *International IRCOBI Conf. on the Biomechanics of Impacts*, (Isle of Man), pp. 353 – 355, 2001.
- [16] D. Baumgartner and R. Willinger, "Human head tolerance limits against impact derived from numerical real world accidents reconstruction," in *7th International Symposium on Computer Methods in Biomechanics and Biomedical Engineering* (J. Middleton and N. Shrive, eds.), 2006.

## **Curriculum Vitae**

Ondřej Jiroušek

### **Education:**

- 1999-2004 Czech Technical University in Prague, Faculty of Civil Engineering (Ph.D.)
- 1993-1999 Czech Technical University in Prague, Faculty of Civil Engineering (M.Eng.)

### **Employer:**

Czech Technical University in Prague  
Faculty of Transportation Sciences  
Department of Mechanics and Materials  
Na Florenci 25  
110 00 Praha 1  
&  
Institute of Theoretical and Applied Mechanics  
Academy of Sciences of the Czech Republic  
Prosecká 76  
190 00 Praha 9

### **Position held:**

Head of the Laboratory of Biomechanics

### **Research Interests:**

- biomechanics of human skeletal system and artificial replacements
- experimental biomechanics
- numerical analysis of biomechanical problems using the Finite Element Method
- parallel processing using linux clusters

### **Teaching activity:**

- since 1999 Czech Technical University, Faculty of Civil Engineering - Elasticity and Plasticity
- since 1999 Czech Technical University, Faculty of Transportation Sciences - Mechanics
- since 1999 Czech Technical University, Faculty of Transportation Sciences - Numerical and Experimental Modelling of Systems in Transportation
- since 2000 Czech Technical University, Faculty of Transportation Sciences - Dynamics

- since 2001 Czech Technical University, Faculty of Transportation Sciences - Elasticity and Strength of Materials
- since 2001 Czech Technical University, Faculty of Transportation Sciences - OS Linux
- since 2002 Czech Technical University, Faculty of Transportation Sciences - Finite Element Method and Its Applications

**Publications:**

5 articles in national and international journals, 3 chapters in books, 48 conference papers

**Research projects:**

- High resolution microCT FE-models of cancellous bone structure and their application to selected problems in biomechanics Grant Agency of the Czech Republic 103/07/P483 (2007-2009) (principal investigator)
- Innovative Track Systems EU 80/06072 (2007-2012) (co-investigator)